

<https://doi.org/10.1038/s42003-025-08337-9>

Human alveolar macrophage response to *Mycobacterium tuberculosis*: immune characteristics underlying large inter-individual variability



Wolfgang Sadee^{1,13}✉, Ian H. Cheeseman^{2,13}, Audrey Papp¹, Maciej Pietrzak³, Michal Seweryn⁴, Xiaofei Zhou⁵, Shili Lin⁵, Amanda M. Williams¹, Mark D. Wewers⁶, Heather M. Curry⁷, Hao Zhang⁸, Hong Cai⁸, Carine Kunsevi-Kilola⁹, Happy Tshivhula⁹, Gerhard Walzl⁹, Blanca I. Restrepo^{10,11}, Léanie Kleynhans¹², Katharina Ronacher¹², Yufeng Wang⁸, Eusondia Arnett², Abul K. Azad² & Larry S. Schlesinger¹²✉

Mycobacterium tuberculosis (*M.tb*) infection infects human alveolar macrophages (HAMs). In freshly isolated HAMs from 28 healthy adults, we observe large inter-individual differences in bacterial uptake and growth, with tenfold variation in *M.tb* load by 72 h. While *M.tb* infection triggers expression changes of numerous host mRNAs, we examined which genes are most variably expressed (VE genes) between donors, as potential biomarkers of individual tuberculosis (TB) risk. The HAM RNA transcriptome following infection revealed thousands of differentially expressed (DE) genes and differential secretion of 25/27 proteins. Yet only 324 DE genes represent VE genes detected exclusively among DE genes in infected cells. Of 36 DE genes detected at all time points (2, 24, and 72 h), 14 are VE genes, indicating early emergence of the VE gene profile. 9/27 DE proteins following infection were encoded by VE genes. Systems analysis of VE RNAs identified a top-scoring network anchored by IL1B, involved in TB immune response. Independent *M.tb*-HAM transcriptome results from a TB-endemic region show significant overlap in DE genes, including VE genes identified in the main study. Thus, we identify a VE gene network activated upon *M.tb*-HAM infection with high inter-person variability, guiding studies on determining individual risk of *M.tb* infection and/or disease.

Mycobacterium tuberculosis (*M.tb*) is estimated to have infected one-quarter of the world's population, and with an estimated 1.3 million deaths in 2022 from tuberculosis (TB), a continuing worldwide public health problem¹. Since only a fraction (5–15%) of infected individuals progresses to active

TB^{2,3}, we must understand the immunopathogenesis of *M.tb* infection, including host susceptibility or resistance factors, in order to develop effective diagnostic, therapeutic and vaccine strategies tailored to different individuals and populations⁴.

¹Department of Cancer Biology and Genetics, College of Medicine, The Ohio State University, Columbus, OH, USA. ²Texas Biomedical Research Institute, San Antonio, TX, USA. ³Department of Biomedical Informatics, College of Medicine, The Ohio State University, Columbus, OH, USA. ⁴Biobank Lab, Department of Molecular Biophysics, Faculty of Biology and Environmental Protection, University of Łódź, Łódź, Poland. ⁵Department of Statistics, College of Arts and Sciences, The Ohio State University, Columbus, OH, USA. ⁶Department of Internal Medicine, Division of Pulmonary, Allergy, Critical Care & Sleep Medicine, The Ohio State University, Columbus, OH, USA. ⁷QED Biosciences, Inc., San Diego, CA, USA. ⁸Department of Molecular Microbiology and Immunology, South Texas Center for Emerging Infectious Diseases, University of Texas at San Antonio, San Antonio, TX, USA. ⁹DSI-NRF Centre of Excellence for Biomedical Tuberculosis Research, South African Medical Research Council Centre for Tuberculosis Research, Division of Molecular Biology and Human Genetics, Department of Biomedical Sciences, Stellenbosch University, Cape Town, South Africa. ¹⁰Department of Epidemiology, School of Public Health, University of Texas Health Science Center at Houston, Brownsville campus, Brownsville, TX, USA. ¹¹University of Texas Rio Grande Valley, South Texas Diabetes and Obesity Institute, Edinburg, TX, USA. ¹²Mater Research Institute and Australian Infectious Diseases Research Centre, The University of Queensland, Brisbane, QLD, Australia. ¹³These authors contributed equally: Wolfgang Sadee, Ian H. Cheeseman. ✉e-mail: wolfgang.sadee@gmail.com; lschlesinger@txbiomed.org

Aerosolized *M.tb* enters the alveolar lung space where it is phagocytosed by alveolar macrophages (AMs), unique resident cells with a complex immunologic profile, to become an intracellular pathogen. *M.tb* infection activates several macrophage immunobiological pathways involved in phagocytosis, vesicle trafficking, and triggering of inflammatory cytokines, oxidants, and cell death pathways—all processes of innate immunity. Yet, critical factors in the human host that promote or impede *M.tb* infection and progression to TB remain uncertain—a roadblock to understanding an individual’s susceptibility to TB^{5–7}.

The host response to *M.tb* infection ranges from complete clearance of infection to latent, incipient, subclinical and active TB⁸. Therapy and vaccine trials further highlight response variability across individuals and populations^{4,9} with BCG vaccination trials attaining only 50% efficacy¹⁰. Evolutionary adaptation of *M.tb* to the host is considered a main factor modulating virulence, host response and TB severity^{11,12}. For example, evasion of immune surveillance by suppression of IL1B was proposed to be largely dictated by virulence of the *M.tb* strain¹¹; however, expression of differentially expressed (DE) genes, including *IL1B*, during infection with a single *M.tb* strain, can vary >10-fold between individuals¹³. Therefore, both genetic¹⁴ and environmental/epigenetic^{15–18} host factors also play a role, while being less well understood.

Heritability estimates of susceptibility to TB range from 80% (twin and population studies) to 25–50% (polygenic risk scores)¹⁹; yet, GWAS-significant genetic variants alone fail to account for most of the estimated heritability^{19,20}. Both in vitro and in vivo transcriptome studies of *M.tb*-infected macrophages and other immune cells reveal candidate genes^{21–24} and associated gene networks^{6,16,25–27}, including type I IFN-associated signatures in active TB, as potential biomarkers^{24,28}. Similarly, protein studies invoke factors associated with TB status, including indoleamine oxidase 1 (IDO1), a blood-based biomarker of active TB²⁹. Complexity of these interacting processes confounds predictions of individual TB risk.

Our study addresses a critical gap in the field, the poorly understood substantial inter-individual variability in response to a single *M.tb* strain in human AMs (HAMs). We address this by characterizing immune response genes and pathways that differ between individuals during infection of HAMs from healthy donors. We identify a set of host DE genes with highly variable expression between HAM donors (VE genes). These VE genes form networks, and we identify hub genes enriched with already recognized biomarkers of active TB^{11,24,29–31}. The enrichment of TB susceptibility genes among the detected VE genes in infected HAMs supports a framework for understanding individual differences in the outcomes of *M.tb* infection, including TB risk or protection, focusing on key genes displaying signatures of evolutionary selection. This study sets the stage for future studies designed

to understand different host responses to distinct *M.tb* strains, vaccines, and therapies.

Results

Heterogeneity in *M.tb* uptake, adaptation and growth in HAMs among donors

We isolated HAMs from 28 adult healthy donors of both sexes and four different races (Table 1) and, within 6 h, infected them with a virulent *M.tb* strain (H₃₇R_v, lineage 4), engineered to emit light (expressed in relative luminescence units, RLUs)^{32–35}. After 2 h, we washed the infected cells and then measured RLUs over 72 h (Fig. 1; Supplementary Table 1). Given the focus of this study on host variation in response to infection rather than *M.tb* strain differences, we selected a single, well-studied strain (H₃₇R_v). The assays presented throughout were conducted at a multiplicity of infection (MOI) of 2:1 or 10:1 (*M.tb*/HAM cells), and macrophage monolayers were maintained throughout the assays. RLUs correlate with *M.tb* colony forming units (CFUs) over time, jointly reflecting the number of intracellular bacilli and microbial metabolic activity^{33–35}. RLU levels at 2–24 h post-infection largely reflect *M.tb* cellular uptake, metabolic activity, and early intracellular adaptation while increases from 24 to 72 h most accurately reflect changes in abundance (growth) of metabolically active intracellular *M.tb*. Similar fold increases in RLUs were observed when HAMs were infected at both MOIs of 2:1 and 10:1 (Supplementary Table 1). After correcting batch effects, large inter-individual variations in RLU values were detectable at each time point (Fig. 1B). HAMs from different donors with the highest and lowest RLUs displayed a nearly tenfold difference at 72 h.

HAM-secreted proteins capture the immune response to *M.tb* infection

To assess the inflammatory mediator response by macrophages to *M.tb* infection, we measured 27 secreted proteins, previously implicated in cellular responses to *M.tb* infection, in all HAMs over 72 h (Supplementary Table 2). Among the secreted proteins 25/27 (92.6%) displayed significantly increased secretion with infection over the 72 h time period with only MMP1 and CCL4 not showing a significant increase in at least one time point (Fig. 2). Even at 2 h, 3 proteins (11%) displayed significantly increased secretion after *M.tb* infection (CCL3, CSF2 and MMP2; Fig. 2). Conversely, 4 proteins (CCL22, IL7, IL16, MMP9) did not show a significant difference until 72 h. Inflammatory mediators including IL1B, TNF and IL6 displayed significantly increased secretion with infection at 24 h and 72 h, consistent with their important contribution to a pro-inflammatory response to infection. Early protein secretion over the first 2 h of infection could influence transcription profiles over the entire incubation period, to be presented further below.

Table 1 | Donor demographics of HAM samples used in this study (n = 28)

Donor	Sex	Age (years)	Race	Donor	Sex	Age (years)	Race
D1	Female	24	Asian (Chinese)	D15	Male	18	Hispanic
D2	Male	24	African-American	D16	Female	25	Caucasian
D3	Male	27	Caucasian	D17	Female	20	Caucasian
D4	Female	26	Caucasian	D18	Female	26	Caucasian
D5	Female	26	Caucasian	D19	Male	19	African-American
D6	Male	21	Caucasian	D20	Female	22	Hispanic
D7	Male	24	Caucasian	D21	Male	20	Asian (Chinese)
D8	Female	22	Caucasian	D22	Female	19	Not stated
D9	Male	23	Caucasian	D23	Female	19	Caucasian
D10	Male	21	Caucasian	D24	Male	23	Caucasian
D11	Female	46	Caucasian	D25	Male	24	Hispanic
D12	Female	22	African- American	D26	Male	23	Caucasian
D13	Male	27	Asian (Indian)	D27	Female	20	Caucasian
D14	Male	33	Asian (Chinese)	D28	Female	19	Caucasian

Male/Female = 14/14; Caucasian = 60% (17/28), Asian = 14% (4/28), African American = 11% (3/28), Hispanic = 11% (3/28). All donors were non-smokers.

Fig. 1 | Time course of *M.tb* interaction with HAMs and intracellular growth over 72 h.

A Schematic of *M.tb* cell attachment and uptake, adaptation, and growth in HAMs. **B** Changes in normalized RLU values over the course of *M.tb* infection. The RLU values represent mostly uptake and adaptation at 2 h and 24 h, and growth at 48 h and 72 h (see Supplementary Table 1; results shown here are with bacterial MOI of 2:1).

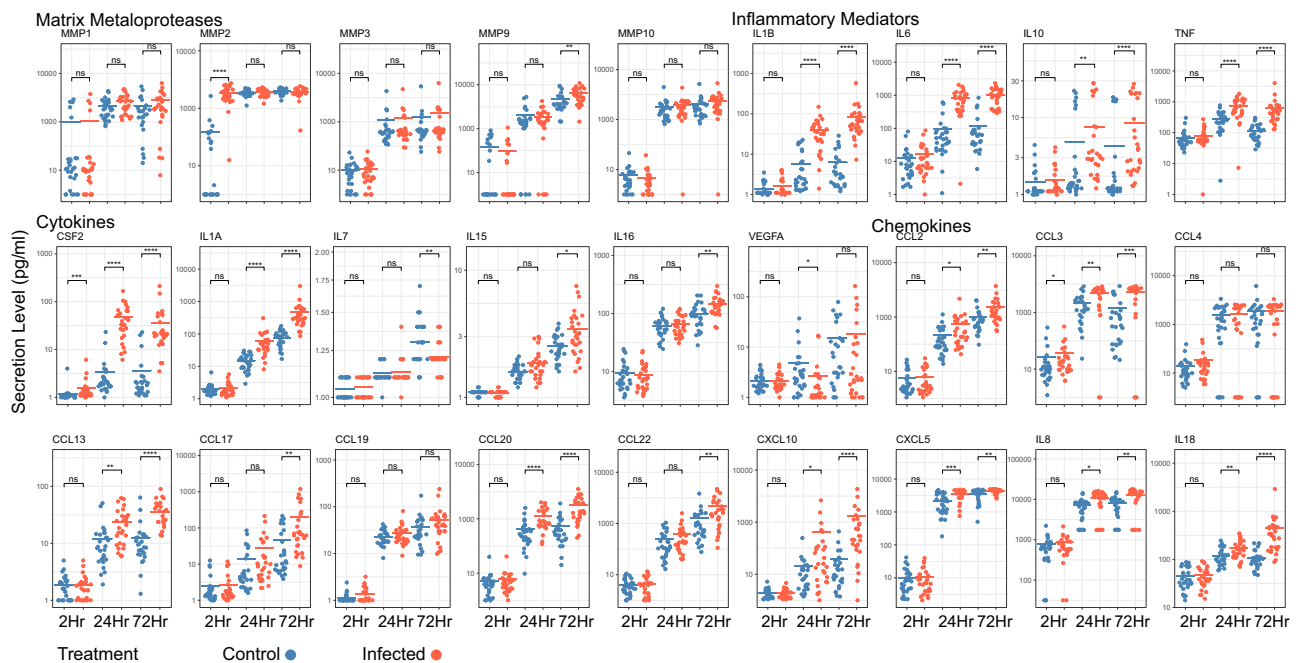
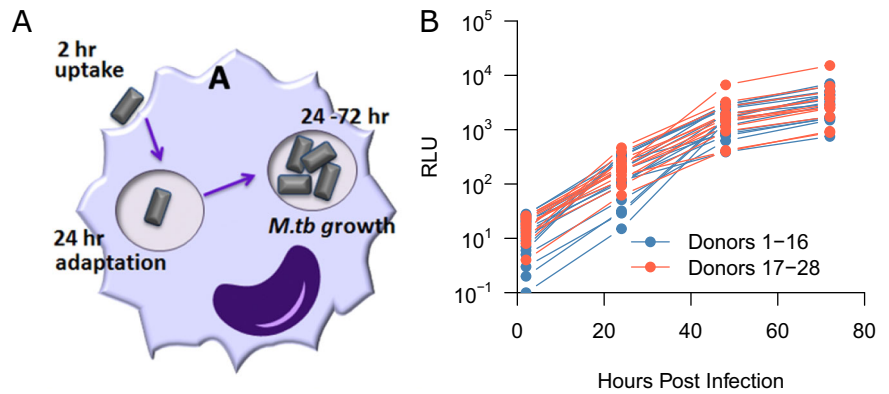


Fig. 2 | Levels of secreted proteins in 28 control and *M.tb*-infected HAMs at 2, 24, and 72 h post infection. Significance of differential protein secretion is given as FDR-corrected *p* values from a Wilcoxon test between infected and uninfected cells (*0.05, **0.01, ***0.001, ****0.0001, ns not significant). Significant increase in

secretion with infection at any of the three time points occurs with 2 MMPs, 4 inflammatory mediators, all 6 cytokines, and 10 chemokines. At 2 h, MMP2, CCL3 and CSF2 are significantly increased in secretion, each also encoded by VE genes, discussed later.

Transcriptomes of uninfected control and *M.tb*-infected HAMs reveal DE gene profiles

Transcript profiles were assessed for each HAM sample with and without *M.tb* infection at 2, 24, and 72 h post infection using AmpliSeq³⁶. This method is scalable across a large concentration range³⁶. At each time point, 10,000–14,000 mRNAs were detectable. Reads per million (RPM) from replicate assays were highly correlated ($r^2 \geq 0.99$), enabling sensitive detection of DE genes.

A principal component analysis (PCA) of all datasets from control and infected HAMs revealed that 52% of the variance in gene expression between time points resulted from exposure of HAMs to ex vivo culture conditions alone, while *M.tb*-induced RNA expression changes were smaller but increased over time (Supplementary Fig. 1). While ex vivo culture alone altered gene expression profiles at 24 and 72 h, infected samples were clearly distinguished from uninfected control samples at each time point by PCA of gene expression (Supplementary Fig. 1). Ex vivo cultured HAMs begin to display a transcriptional profile of ex vivo differentiated monocyte-derived macrophages (MDM) after 6 h incubation³⁶, further supported by the dataset explored in this study (Supplementary

Fig. 2). Canonical HAM markers were highly expressed at 2 h in both control and infected samples. These markers included SERPING1, LGALS3BP, MRC1, MARCO, MCL1, HLA-DQA1, CCL18, CES1, TREM2, A2M, MMP7, CD84, MMP9, CD36, NOS2, IL18, CCL8, CCL5, IL23A, CD40, CCL3, CCL4, IL1B, TLR2, CD80, FCGR2A, SOCS3, TNF, CD86, FCGR1A, FCGR3A, IL12A, TLR4, IL1R1, CCL11, IL13, VEGFA, IL10, TLR8, CD200R1, CCR2, TLR1, CD68, CCL22, CCL1, CCL17, CCL24, ARG1, IL4, PPARG, CD163, and TGFBI.

To identify significant DE genes (FDR adjusted $p \leq 0.05$) specific to infection, we analyzed RNA expression by comparing uninfected control cells to infected cells at each time point. This yielded 62 DE genes at 2 h, 2,177 at 24 h, and 3662 at 72 h post infection (Supplementary Table 3)³⁶. Thirty-six genes were significantly DE at all time points, all but 2 were upregulated (Figs. 3A and 4), including those encoding inflammatory cytokines (IL1A, IL1B, TNF) and chemokine receptors (e.g., CCR7) characteristic of a spectrum typically reported as representing “M1 type” cell states, and GPR84, a regulator of macrophage functions³⁷.

Macrophage polarization is often simplified to the trajectory towards M1-like or M2-like states, the former representing a pro-inflammatory

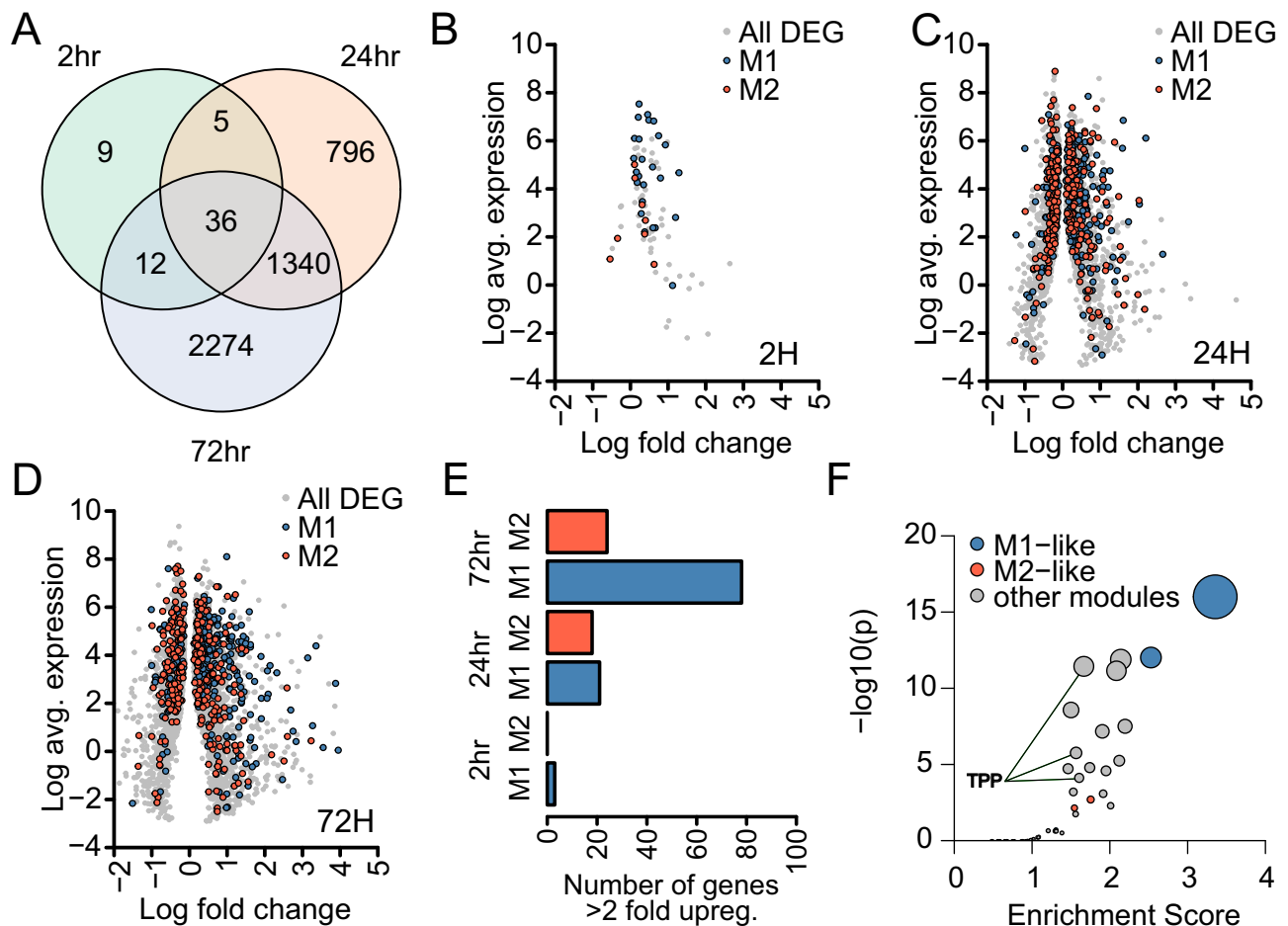


Fig. 3 | The transcriptional response to *M.tb* infection by 28 HAMs. A Venn diagram of differentially expressed (DE) genes between *M.tb*-infected and uninfected controls at three time points. Total number of genes with detectable expression (≥ 1 RPM) was $\sim 12,000$. DE genes were detected with DESeq2 (adjusted p values < 0.05): 62 at 2 h, 2177 at 24 h, and 3662 at 72 h, with overlaps displayed in the Venn diagram. Log₂ fold change and log₂ average expression for DE genes at 2 h (B), 24 h (C) and 72 h (D). M1 and M2 genes are shown in blue and red, respectively.

E The number of DE genes with >2-fold upregulation defined as 'M1-like' or 'M2-like'. This uses an independent definition of 'M1-like' and 'M2-like' genes to (F). F Gene set enrichment analysis of DE genes from 72 h using 48 gene expression modules previously determined as operational in macrophage differentiation. Modules annotated as 'M1-like' or 'M2-like' are shown in blue and red, another major grouping of modules was related to ex vivo TPP (TNF, PGE2 and P3C) stimulation in macrophages⁴⁰ and are highlighted by a line.

state³⁸. To explore the relevance of these polarized states to differences between control and infected samples, we first assessed changes in the abundance of M1- and M2-associated mRNA transcripts between control and infected cells (Supplementary Fig. 2) using a curated set of M1- and M2-associated genes³⁹. There was a substantial overlap between DE genes at each time point and M1/M2 genes (Fig. 3B–E), with 44.0% of M1 genes and 34.0% M2 genes differentially expressed at 72 h. An independent analysis supported the importance of M1/M2 genes. Gene set enrichment analysis of 72 h DE gene profiles, using gene co-expression modules previously identified during macrophage differentiation⁴⁰, showed significant enrichment of M1-like modules (Fig. 3F). While our data supports the relevance of 'M1'-like states to *M.tb* infection, they also indicate that macrophages are not simply M1 or M2. Polarization into either 'M1' or 'M2'-like states is increasingly recognized as a false dichotomy with macrophages actually residing across a spectrum of states^{41–44}.

DE genes display the most variable expression in HAMs between donors (VE genes)

The analysis of DE genes across all HAM donors does not identify genes that reveal variable expression between individuals – the principal goal of this study. For example, induction of the highly significant DE transcript STAT1 (a transcription factor associated with an M1-like state) varied between HAM donors from a 2-fold reduction to a 25-fold increase. To capture inter-

individual variation, we analyzed variance of gene expression in both control and infected HAMs at all time points combined, yielding a set of 324 genes with highly variable expression, exclusively found in *M.tb*-infected HAMs (VE genes; Levene's test, ratios of variances ≤ 0.15 ; Supplementary Table 4A). Considering the lack of VE genes in control HAMs, their emergence in infected HAMs supports the notion that *M.tb* infection causes highly variable gene expression.

All 324 VE genes are also significant DE genes which were upregulated in the *M.tb*-infected HAMs. Examples include *IFI6*, *IL1B*, *CCL4*, *IDO1*, *GBP5*, *IRF1*, *JAK3*, *UBD*, *CXCL5*, *CCL20*, *VDR*, *CD80*, *IFI44L*, *NLRP3*, and *IL7R*, several previously implicated in TB pathogenesis [reviewed in refs. 19,45]. Among the 27 secreted candidate proteins measured, 9 also scored as VE gene-encoded proteins (*CCL2*, *CCL3*, *CCL4*, *CCL20*, *CCL22*, *CXCL5*, *IL1A*, *IL1B*, *MMP2*). Moreover, among the 36 genes differentially expressed at all time points, 14 were VE genes (*AMPD3*, *CCL2*, *CCL4*, *CCL20*, *CXCL1*, *CXCL5*, *F3*, *GOS2*, *GPR84*, *IL1A*, *IL1B*, *NBN*, *PTX3*, *TNFAIP6*), indicating that a unique individual mRNA pattern is established as early as 2 h after infection.

Among the VE genes, a subset of them was tightly co-expressed with *IDO1*, displaying extreme variability between HAMs, including *IL1B*, *CCL5*, *GBP2*, *IFI44L*, *IRF1*, *JAK3*, *STAT1* and *UBD* (Fig. 5). For example, *IDO1* [a well-characterized TB marker²⁹] was expressed over a large range of RPMs, with only a portion of HAMs showing substantial expression (well above

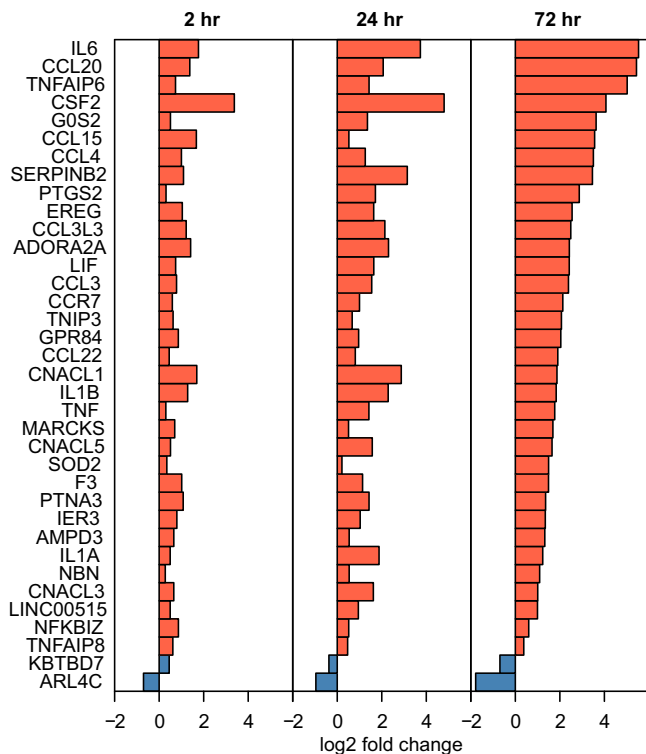


Fig. 4 | The transcriptional response of 28 HAMs to *M.tb* infection. Shown are the 36 significant DE genes common to all time points (see Fig. 3A), and their average \log_2 fold change.

500 RPMs) at 24 h (Fig. 5B–H), while *IL1B* was more broadly expressed, but with high expression mostly coinciding with high *IDO1* expression at 72 h (Fig. 5A). VE genes with large differences in expression between HAM donors are primary candidates for potential relevance to individual susceptibility to TB. Since several VE gene transcripts are formed and multiple VE proteins (CCL3, MMP2, CSF2) are secreted within 2 h of *M.tb* infection (Fig. 2), it appears that large inter-individual differences in cellular HAM response to *M.tb* infection emerge almost immediately.

Reactome analysis of the 324 VE genes yielded several significant pathways, including Immune System and Cytokine Signaling (Supplementary Table 4B). Ingenuity Pathway Analysis (IPA) of the VE genes yielded the highest scoring hierarchical network with *IL1B*, *IRF1*, *IDO1*, *STAT1* and *UBD* as main hub genes with many connections, and secondary hub genes with 4 or more connections (CCL2, CD40, CD80, CD274, CFB, CXCL3, GBP2, IL1A, IL1RN, OSM, PSMB2, PSMB8, STAT2, TRL2, TNFRSF4, TNFRSF10, USP18) (Fig. 6, full gene annotation in Supplementary Fig. 3). Both *STAT1* and *IRF1* interact with the *IDO1* promoter⁴⁶ and play a role in macrophage polarization and may therefore represent biomarker candidates affecting inter-individual variability in response to HAM infection.

These combined analyses reveal VE genes meeting multiple criteria as potential candidate biomarkers linked to individual TB susceptibility: differential expression upon infection, high interindividual variability in expression, member of a critical gene network, and previous evidence for TB biomarker status.

Relationships between protein secretion at 2h and transcript profiles of VE genes

Among the 27 proteins measured (Fig. 2), 25 were encoded by DE genes, and 9 by VE genes (CCL2, CCL3, CCL4, CCL20, CCL22, CXCL5, IL1A,

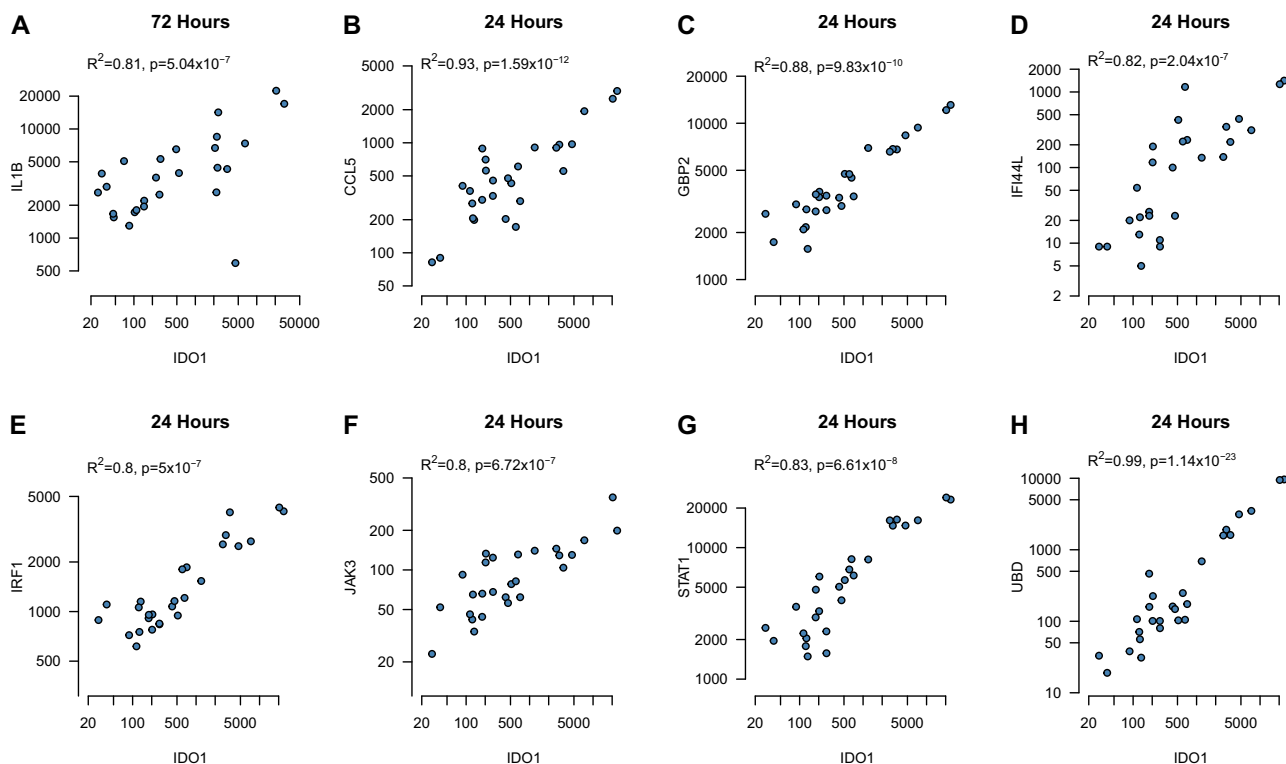


Fig. 5 | Expression of *IDO1* compared to *IL1B* and other co-expressed genes in HAMs infected with *M.tb* at 24 or 72 h. A Expression of *IDO1* compared to *IL1B* at 72 h: both are variably expressed with a similar pattern across the 28 HAMs ($R^2 = 0.81$). B–H Select mRNA transcripts with co-expression patterns highly

correlated with *IDO1* at 24 h ($R^2 \geq 0.80$). *IDO1* is expressed in all HAMs over a wide range of scales in reads per million (RPM), with examples of the most tightly co-expressed genes with *IDO1* representing the most variably expressed gene cluster (B–H). Gene expressions are shown in RPM on both axes.

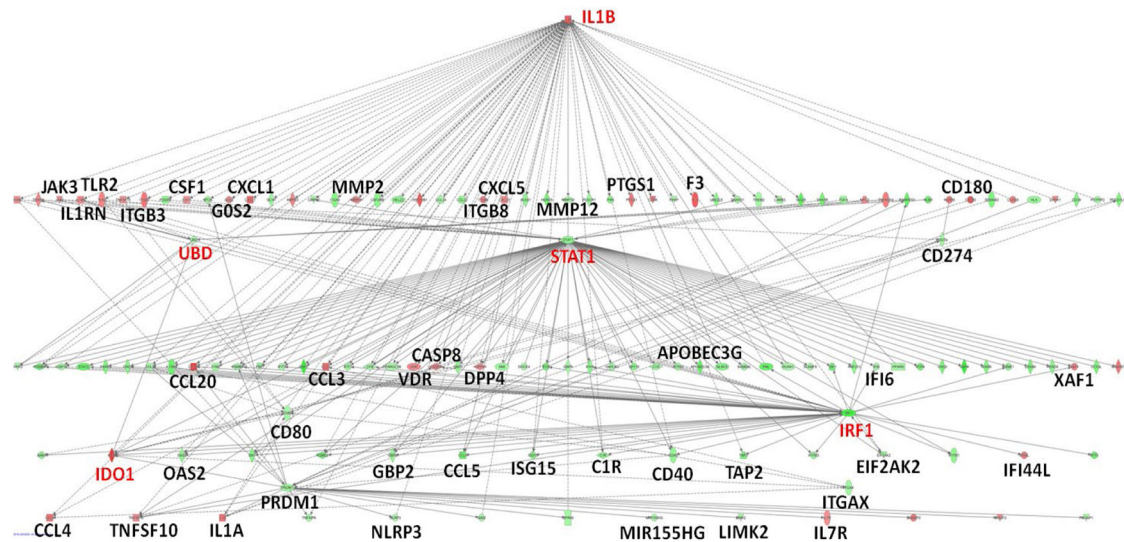


Fig. 6 | Network of DE genes with highly variable RNA expression (VE/DE genes). These VE/DE genes ($n = 324$) were identified in the 28 HAMs after *M.tb* infection across all time points. Standard pathway enrichment program, Ingenuity Pathway Analysis (IPA) ([https://www.qiagenbioinformatics.com/products/ingenuity-](https://www.qiagenbioinformatics.com/products/ingenuity-pathway-analysis/)

[pathway-analysis/](https://www.qiagenbioinformatics.com/products/ingenuity-pathway-analysis/)), generates a top scoring gene network with *IL1B*, *UBD*, *STAT1*, and *IRF1* as key hub genes. *STAT1* and *IRF1* co-operatively bind to the promoter of *IDO1*, another hub gene, which is also highlighted (fully annotated network is depicted in Supplementary Fig. 3). These key proteins are highlighted in red.

IL1B, *MMP2*). This overlap supports the selection of these proteins as candidates for a role in individual donor-*M.tb* interactions. Differential secretion of proteins can result from direct effects of *M.tb* on cellular metabolism, increased transcription, translation, and secretion, or as a result of secondary autocrine/paracrine effects of the secreted proteins themselves. To test this early in the infection, we assessed how changes in secreted protein levels in control and infected HAMs at 2 h post *M.tb* infection correlate with mRNA expression at 2, 24, and 72 h (Supplementary Table 5). We focused on mRNAs encoded by VE genes to determine at what point the VE gene profile and gene network are activated. The correlation pattern between secreted proteins at 2 h and VE transcripts revealed robust correlations already at 2 h and more robustly at 24 h and 72 h post infection, shown in Fig. 7 for VE transcripts at 24 h. Strong correlations (R up to 0.6 and $FDR\ p < 0.01$) were observed between several proteins with multiple VE mRNAs for both control and infected HAMs. Significant correlations were found either in the controls or in infected HAMs, or in both. For example, 2 h protein levels of *CCL2,3,20*, *CSF2*, *CXCL10,11* and *IL6,8* correlated positively with *IFITM1-3*, *GBP3*, *OAS*, *ISG20*, and *IRF1* transcripts at 24 h in infected cells (Fig. 7, see lower left and right panels). The correlation between 2 h *CCL3* protein and 24 h *ISG20* transcripts was significant in infected HAMs ($R = 0.56$, $FDR\ p = 0.0003$) but not in controls ($R = 0.09$, $FDR\ p = 0.26$). The same proteins correlated with another set of mRNAs more strongly in the control cells, indicating that infection reverses changes incurred from incubation of cells alone (e.g., *VDR*, *C1RF*, *CSF1*, *CCL24*) (Fig. 7, lower middle panel). The correlation between *CCL3* and *VDR* was $R = 0.52$ (FDR adjusted $p = 0.07$) in the controls and $R = 0.08$ (FDR adjusted $p = 0.70$) in infected HAMs. Yet other proteins displayed only modest changes in correlations between controls versus infected HAMs (e.g., *CCL20*, *IL13*, 17, 19). These results demonstrate that *M.tb* infection causes rapid rewiring of protein secretion and expression of VE genes already at 2 h of infection with distinct differences compared to changes caused by incubation alone for a subset of VE gene transcripts. Moreover, these results support the hypothesis that early protein secretion plays a role in determining individual cellular responses to *M.tb* infection over time, exerting autocrine or paracrine stimuli that further enhances early evolution of the VE gene network.

Among the secreted proteins, robust release of *MMP2* into the medium occurred in the absence of any changes in *MMP2* mRNA levels at 2 h, unique among all other proteins tested (Fig. 2; Supplementary Tables 2, 3A). *MMP2* mRNA was stimulated by *M.tb* only at 24 and 72 h.

MMP2 protein levels at 2 h post infection correlated with several transcripts at 24 h only in the infected cells: *VDR* ($R = 0.43$, $FDR\ p = 0.03$), *IL1B* ($R = 0.59$, $FDR\ p = 0.01$) and *CCL20* ($R = 0.54$, $FDR\ p = 0.004$) (Supplementary Table 5), suggesting a downstream effect on *M.tb*-HAM interactions.

Replication study of freshly isolated HAMs in a different population using RNA-Seq

To determine whether the HAM DE or VE genes identified in our primary cohort would be seen in a replication cohort, we applied full RNA sequencing in HAM samples infected similarly with *M.tb* H₃₇R_v from a different population in South Africa. This population included 9 donors used as healthy controls with QuantiFERON positive status (Table 2), where all donors did not have HAM samples from all 3 time points of infection (2 h, 24 h, 72 h). Analysis of the RNA sequencing data yielded a set of DE genes that overlapped with those in HAM samples of our primary study. DE genes are presented in Supplementary Tables 6A–C, and Supplementary Fig. 4. At 2 h post infection, fewer RNAs were assigned DE status ($n = 45$), and only 3 upregulated RNAs overlapped with the DE genes in the primary study, likely owing to the small number of samples and the less precise and less targeted RNA-Seq methodology. However, at 24 h, 360 of 773 DE genes (46.6%), and at 72 h, 89 of 148 DE genes (60.1%) overlapped with the DE genes reported in the main study. Pathway analyses revealed a similar spectrum of enriched functional terms for upregulated genes, including cytokine signaling in immune system, interferon signaling, and innate immune system (Supplementary Tables 6D, E). Inspection of key DE genes, irrespective of HAM donors and infection time points, replicated the finding of substantial inter-individual differences, for example *IDO1* and its co-expressed genes (Supplementary Fig. 5). We next sought to determine the overlap between VE genes in the larger 28 HAM panel of the main cohort with DE genes in the South African samples (Supplementary Fig. 6). However, owing to the smaller sample size, a direct variance analysis to define VE genes was not considered viable, while overlapping with DE genes in the replication cohort provided a measure of VE gene expression. Since the mean expression of all VE genes was upregulated in the main study, we considered only upregulated DE genes in the replication study. This analysis revealed that VE genes are enriched among the DE genes at 24 and 72 h, representing more than 34% of all upregulated DE genes at 72 h (45 of 131). This result is a further indication that VE genes are an important component of the transcriptome response to *M.tb* infection.

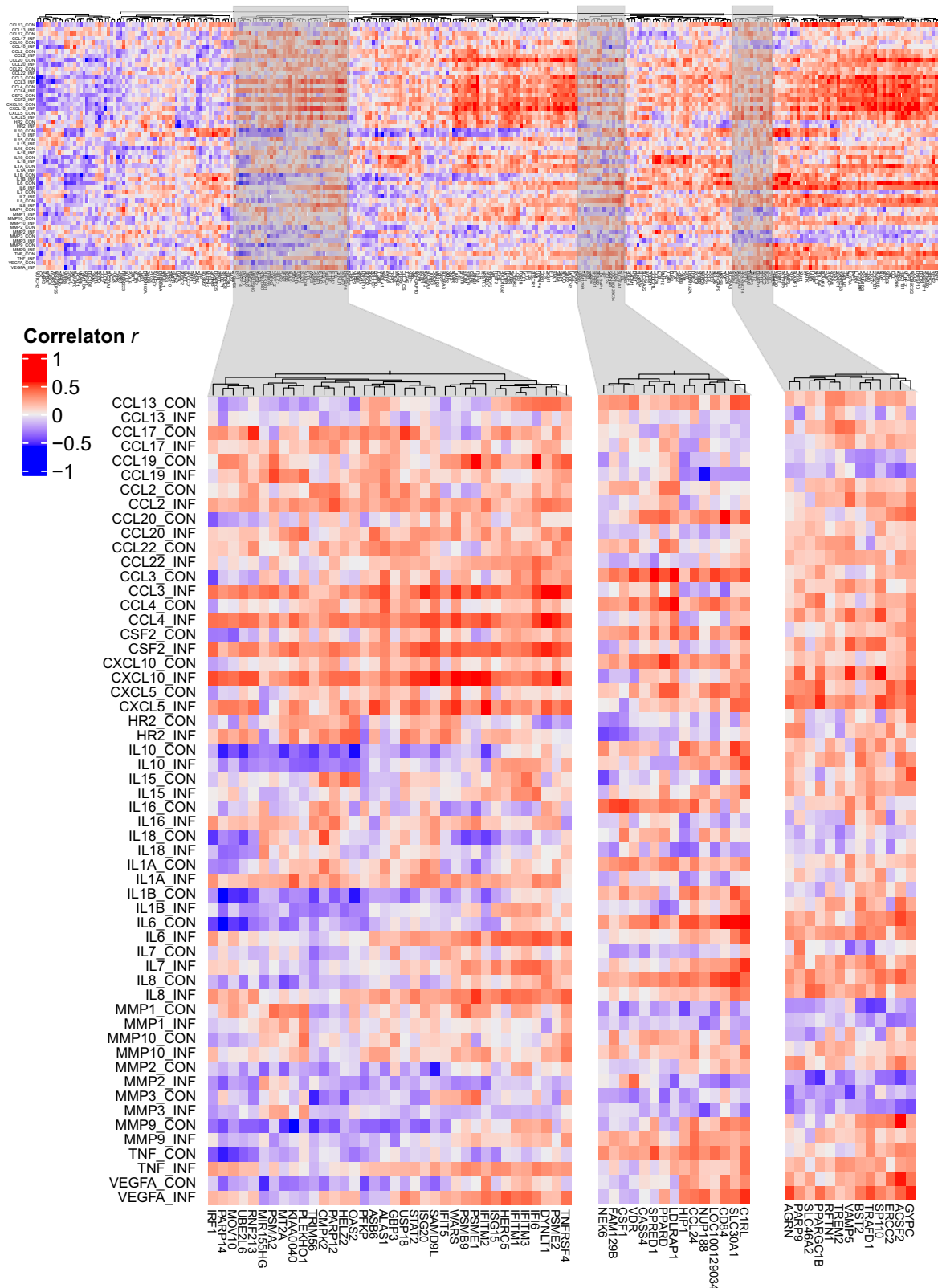


Fig. 7 | Heatmap of correlations between secreted protein levels (y-axis, $n = 27$) in control and *M.tb*-infected HAM incubations at 2 h post *M.tb* infection versus cellular VE mRNAs 24 h post *M.tb* (x-axis, $n = 324$). This heatmap illustrates potential effects of early secreted proteins on subsequent mRNA levels at 24 h, indicating potential autocrine/paracrine effects. A clear pattern of enhanced correlation of proteins (e.g., CCL3/4, CSF2, CXCL5/10, IL6) with mRNA expression encoded by several VE gene transcripts (e.g., IRF1, IFI6) is visible, highlighted in the

lower expanded sections on the left and right. However, the same proteins display the opposite trend with higher correlations in the control cells (e.g., C1RL, CSF1, CCL24) (gene transcripts in the lower middle section). Other proteins do not show such a pattern (e.g., IL10) or even opposite correlations throughout (e.g., IL13, IL7, and IL19). All data are in Supplementary Table 5, including all correlations between 2 h protein levels and 2, 24, and 72 h mRNA levels). For a high-resolution version of the top of figure inset, please see Supplementary Fig. 7.

Table 2 | Healthy control demographics of South African HAM samples used for replication study (*n* = 9)

Donor ID sex ^a	Age (years)	Smoker race ^b	RNA-seq samples ^c 2 h 24 h 72 h
A257 (LS_109-120) Female	62	Yes SAC	No Yes Yes
A258 (LS_121-126) Male	51	Yes SAC	Yes Yes Yes
A316 (LS_141-148) Female	46	Yes SAC	Yes Yes Yes
A335 (LS_149-158) Female	47	Yes SAC	Yes Yes No
A352 (LS_161-166) Female	43	No SAC	Yes Yes No
A367 (LS_169-174) Female	58	No SAC	Yes No No
A411 Female	62	No SAC	Yes No No
A415 (LS_177-182) Female	53	Yes SAC	No No Yes
A416 (LS_183-184) Female	52	No SAC	Yes No No

^aThe designation in parenthesis refers to a range of RNA sample numbers obtained under different conditions from the same donor used for RNA-seq.

^bSAC: South African Colored (mixed ancestry with Khoisan, Bantu, European and Asian roots).

^cHAM samples from three different time-points of infection available for RNA-seq.

Discussion

This study highlights substantial inter-individual variation in the transcriptomic and proteomic response to *M.tb* infection of HAMs from healthy human donors. Using a single virulent *M.tb* strain, and in the absence of comorbidities, our results define a gene network with tight co-expression and high variability (VE genes) between HAM donors. Application of the high precision AmpliSeq RNA assay enabled detection of numerous significant DE RNAs across the 28 donors for HAMs³⁶, similar to previous results^{24,31}. To focus on genes likely to affect *M.tb* interactions with HAMs, we performed variance analysis to identify a smaller set of 324 VE genes between donors (Supplementary Table 4). All VE genes were also DE genes present only in infected but not control HAMs, indicating that the VE profile was a specific response to *M.tb* infection and thus represents potential key factors in determining an individual's cellular response to *M.tb*. VE genes have previously been proposed as markers of individual susceptibility or resistance to disease phenotypes⁴⁷. The VE gene set emerged as early as 2 h post *M.tb* infection and contained multiple genes previously implicated in TB pathogenesis. Supporting these conclusions, a smaller replication study with HAMs obtained from a South African cohort identified an overlapping set of DE genes that also included a substantial share of VE genes identified in the main study (Supplementary Table 6 and Supplementary Figs. 4–6).

Analysis of the VE genes yielded a top scoring gene network with *IL1B* as anchor (Fig. 6). Sousa et al.¹¹ had demonstrated that secretion of *IL1B* is a surrogate marker distinguishing between mild and severe TB disease, attributing differences in *IL1B* induction to virulence of the strains tested, independent of the host. Both laboratory and clinical strains of *M.tb* have been shown to induce increased production of caspase-1 independent *IL1B* which could clear the bacterial burden from infected animal lungs. Thus, *IL1B* plays a major role in host defense to *M.tb*^{48,49}. Here we show that a single virulent *M.tb* strain elicits substantial differences in *IL1B* expression between individual HAM donors, along with additional associated candidate genes, indicating that preexisting host factors could potentially serve as predictive markers of TB susceptibility.

Parallel analysis of 27 selected candidate proteins secreted by HAMs revealed significant stimulation by *M.tb* of all but 2 proteins (Fig. 2), also with substantial inter-subject variability (Supplementary Table 2). Nine of these proteins were encoded by VE genes (*CCL2*, *CCL3*, *CCL4*, *CCL20*, *CCL22*, *CXCL5*, *IL1A*, *IL1B*, *MMP2*), highlighting potential relevance as individual biomarkers of host susceptibility. Robust correlations between proteins secreted during the first 2 h post infection and VE gene expression at later time points (Fig. 7 and Supplementary Table 5) suggest autocrine and paracrine mechanisms contributing to the cellular response to *M.tb*. Secretion of *MMP2* at 2 h occurred in the absence of increased mRNA expression, consistent with release of pre-formed *MMP2* from the cell during bacterial attachment. Matrix metalloproteinases are known to be upregulated by *M.tb* infection, degrading the extracellular matrix and thereby affecting cellular infectivity⁵⁰; hence the level of *MMP2* secretion could serve as an early distinguishing factor in *M.tb* infection. Further proteomic and metabolomic studies could reveal early rapid cellular mechanisms of differential HAM responses during *M.tb* attachment and cellular uptake. These earliest interactions with HAMs at the cell surface play an underappreciated role in regulating subsequent effects during the intracellular residence of *M.tb* [so-called step 1⁵¹].

Reactome and IPA analyses of VE genes yielded Immune System and Cytokine Signaling in the Immune System as the top pathways (Supplementary Table 4B). The top-scoring network with *IL1B*, *STAT1*, and *IRF1* as dominant hubs (Fig. 6; Supplementary Fig. 3) included genes previously implicated in the cellular response to *M.tb* [e.g.,^{23,24,31}]. The VE gene product *GBP2* is an IFN/*IL1B* activated GTPase mediating antibacterial defense, one of the genes in the blood-based RISK6 transcriptome proposed as a biomarker for TB disease and treatment response⁵². This *IL1B*-dominated network connects *STAT1*, and *IRF1* to *IDO1* (Fig. 6), consistent with previous reports that the *IRF1/STAT1* transcription complex binds to the *IDO1* promoter^{46,53}. *IDO1* has been proposed as a sensitive and selective biomarker for active TB²⁹. Its metabolic products, immunosuppressive kynurenins, act by preventing access of cytotoxic T cells to infected macrophages in TB lung granulomas³⁰. *IDO1* is encoded by a key VE gene robustly expressed in only 8–10 of 28 HAMs after *M.tb* infection (Fig. 5A), with a highly correlated expression profile with *CCL5*, *IL1B*, *IFI44L*, *UBD*, *STAT1*, *IRF1*, *JAK3* and *GBP2* (Fig. 5). Further proteins encoded by VE genes relevant to *M.tb* pathogenesis include *UBD* and *GPR84*. Ubiquitin pathways, including *UBD*, mediate cellular responses to intracellular pathogens by modulating autophagy and pyroptosis^{54,55}. The phosphatase *PtpB* from *M.tb* requires ubiquitin binding to inhibit the host inflammasome-pyroptosis pathway. Since disrupting *PtpB* activity reduces intracellular pathogen survival, highly variable *UBD* expression levels in host cells likely play a role in *M.tb* infection and survival in HAMs. Similarly, the short chain fatty acid sensor *GPR84* can enhance pro-inflammatory responses, bacterial adhesion and phagocytic activity of macrophages, thus playing a key role in macrophage responses³⁷. We propose that *M.tb*-induced expression of these VE genes could be early predictive indicators of susceptibility to *M.tb* for a given individual. In future studies, this hypothesis can now be addressed in readily accessible cells [e.g., Alveolar Macrophage-Like (AML) cells, derived from blood monocytes], recently published as a surrogate for HAMs, which maintain a HAM-like phenotype over days in culture^{44,56–58}].

Although macrophages were initially characterized as having polar phenotypes, i.e., M1 or M2⁵⁹, HAMs represent a unique spectrum of phenotypes with both M1 and M2 markers⁴³. Thus, as expected, employing published modules³⁹ defining classical M1 or M2 type genes, we find that upregulated genes represent both activated M1 and M2 types (Fig. 3). A previous study reported that *M.tb* ESAT-6-induced macrophage polarization to an M1 phenotype occurred early and then switched to M2 phenotype at a later stage of infection⁶⁰. Differences in the baseline level of expression of M1 and M2 marker genes could account in part for inter-individual differences in *M.tb*-AM interactions that control the fate of *M.tb* in these cells.

In conclusion, our results identify key genes and their encoded transcripts and proteins in the early phase of *M.tb* infection of freshly

isolated HAMs from healthy donors that are expressed with high variability between individual donors, a potential characteristic of disease-associated genes. Many of these VE genes have been shown to play a role in TB pathogenesis. Variations between individuals in VE genes underlie alterations in common pathways that play a fundamental role in pathogenesis. We postulate that a focus on VE genes and their associated co-expressed gene modules can serve as a foundational approach for identifying early predictive biological indicators of an individual's susceptibility or resistance to *M.tb* infection, TB disease progression/severity, and response to therapies and vaccines⁶¹.

Limitations

The current study employs freshly isolated HAMs (used within 6 h of harvest) and hence is distinct from MDMs isolated from peripheral blood after 5 days of in vitro incubation, accounting for substantial differences of RNA profiles between them³⁶. After 2 h incubation, both control and infected HAMs display a strong mRNA expression profile attributable to freshly obtained HAMs, this pattern dissipates over longer incubations (Supplementary Fig. 2), as we have found previously³⁶. To mitigate in vitro artifacts, we infected HAMs within 6 h of harvest and used uninfected HAM controls at each time point for each donor. Whereas the incubation conditions alone induced substantial changes in gene and protein expression, exposure to *M.tb* generated a distinct set of DE genes, many also being VE genes, as early as 2 h of incubation, readily distinguished from control expression profiles and even reversing some changes caused by incubation conditions alone (Fig. 3; Supplementary Figs. 1, 2; Supplementary Tables 3, 4). These findings indicate that early events caused by *M.tb* exposure arise from a state of HAM cells still close to the in vivo state. However, the changing HAM phenotype during the incubation period confounded correlations between gene expression and *M.tb* growth and therefore were not included here.

While the study group of 28 healthy HAM donors was sufficient to reveal significant genes associated with *M.tb*-HAM interactions (this is a relatively large study given the difficulty of obtaining fresh HAMs from healthy individuals), supported by a smaller replication cohort, functional studies will be required to establish causal relationships. Also, larger cohorts will be needed to rigorously address contributions of ethnicity and genetics, sex, age and environmental factors. Nevertheless, this study provides rich datasets facilitating development of predictive biomarker panels of individual TB risk. The design of our study precluded repeat measures from each donor. However, our longstanding studies with healthy donor human MDMs and HAMs have demonstrated that individual healthy donors provide consistent results for comparable measurements over time.

Methods

Measurements of uptake, adaptation, and growth rate of *M.tb* in infected HAMs

Freshly obtained HAMs were prepared and cultured within 6 h from 28 tuberculin skin test (TST)-negative non-smoking, healthy donors from Caucasians, Asians, and Africans, according to the demographics of the Columbus, Ohio area (Table 1), under an approved IRB protocol at the Ohio State University Wexner Medical Center. The informed consent from each donor was obtained and all ethical regulations relevant to human research participants were followed. Isolation and culture of HAMs from bronchoalveolar lavage (BAL) was done as described^{62,63}. Briefly, BAL fluid was centrifuged and washed once in cold RPMI at 4 °C, and the cell pellet was re-suspended in RPMI medium. A portion of the cell suspension was subjected to cyto-spin followed by HEMA 3 differential staining and microscopy to determine the percentage of macrophages (94 ± 5%; mean ± SD, *n* = 10). HAMs were adhered for 2 h in either a 24-well plate (1.5 × 10⁵ cells/well) or 96-well plate (5 × 10⁴ cells/well) in RPMI containing 10% human AB serum and Penicillin G (10,000 U/ml). The resultant uninfected HAM monolayer was then washed (~99% pure as assessed by phase contrast microscopy), and cultured in RHH media (10 mM HEPES, 0.1% human serum albumin, RPMI) for

another 2 h (this is the time period where *M.tb* was added to separate wells for the infection). Supernatants were collected for protein and cell monolayers lysed for RNA analysis. For longer time points, monolayers were washed, medium replaced, and incubations continued for 24 or 72 h for repeat protein and RNA analysis.

For *M.tb* infection of HAMs, virulent *M.tb* H₃₇R_v single cell suspensions were prepared⁶⁴. The virulent *M.tb* strain used retains PDIMs and contains the entire bacterial Lux operon cloned in a mycobacterial integrative expression vector (*M.tb* H₃₇R_v-Lux) as described^{32,33}. *M.tb* cellular uptake, adaptation, and intracellular growth were assessed as relative luminescence units (RLUs) at 2, 24, 48, and 72 h in 3–5 wells for each condition (mean values of 3–5 technical replicates are provided for each donor) using a multiwell plate reader (Glomax, Promega). Each 2 h incubation was performed at a multiplicity of infection (MOI) of both 2:1 and 10:1 (*M.tb*/HAM cells for RLU assays); RNA and protein were measured only with MOI of 2:1. Cells were imaged daily with a light microscope to assess monolayer integrity, which was maintained throughout the experiment.

For technical reasons, HAM uptake and growth assays from donors 1–16 were incubated in 24 well plates, while HAMs from donors 17–28 were incubated in 96 well plates. Use of the different-sized plates resulted in ~3-fold difference in mean RLUs between the two sets of donor groups (directly related to a different number of HAMs/well and thus bacteria/well). For all analyses we performed batch correction of protein, transcript and RLUs using ComBAT⁶⁵ to remove the impact of different plates used during culture, as such we specified the batches as individuals 1–16 and 17–28.

Measurement of secreted proteins in control and *M.tb*-infected HAMs

Supernatants from culture wells of uninfected and infected HAMs from 28 donors at 2, 24, and 72 h were analyzed for secreted proteins relevant to *M.tb*-macrophage interactions using multiplex kits from Meso Scale Discovery (MSD) (Rockville, MD). The supernatants were collected at 2 h and replaced with fresh medium, followed by continuing incubation until 24 or 72 h. Twenty-seven secreted proteins were measured: 4 inflammatory mediators (TNF-α, IL-6, IL-1β, IL-10; using V-PLEX kit), 6 cytokines [CSF2 (GM-CSF), IL-15, IL-16, IL-1α, IL-7, VEGFA] and 12 chemokines [IP-10 (CXCL10), MCP-1 (CCL2), MCP-4 (CCL13), MDC (CCL22), IL-8, TARC (CCL17), MIP-1α (CCL3), MIP-1β (CCL4), ENA-78 (CXCL5), IL-18, MIP-3α (CCL20), MIP-3β (CCL19); using U-PLEX (customized multiplexing) kit], and 5 matrix metallo-proteinases (MMP-1, MMP-2, MMP-3, MMP-9, MMP-10; using MMP 3-PLEX and MMP 2-PLEX kits).

Measurement of RNA expression from uninfected control and *M.tb*-infected HAMs

Expression of 20,804 RNAs, including 2228 non-coding RNAs (ncRNAs), was measured with AmpliSeq™ (Whole transcriptome Human Gene Expression Kit, Life Technologies) for 28 donor HAMs at 2, 24, and 72 h after infection, for both uninfected controls and infected HAMs at each time point (MOI 2:1). AmpliSeq transcriptome analysis incorporates a targeted, amplicon-based (~110 bps, spanning exons) workflow, and is quantitative over orders of magnitude. The precision of AmpliSeq analysis detects *M.tb*-induced expression changes with high sensitivity in human MDMs and HAMs infected with *M.tb*³⁶. Genomic DNA and total RNA (TRIzol® Reagent (Ambion™, Austin, TX)) were prepared from HAMs using published procedures¹³. RNA was purified, DNase-treated, concentration measured, and its integrity assessed as described³⁶. Reverse transcription of 10 ng total RNA was performed by using the SuperScript® VILO™ cDNA Synthesis kit and the AmpliSeq primers. The cDNAs were amplified for 12 cycles with Ion AmpliSeq™ primers and barcoded adapters, resulting libraries purified and pooled in equal amounts for emulsion PCR on an Ion OneTouch™ 2 instrument, followed by sequencing with the Ion Proton™ sequencer³⁶. Reads were aligned to BED (Browser Extensible Data) file specific for AmpliSeq amplicons. Typically, we obtained 5–9 million mappable reads per

sample, with ~50–60% of RNA targets detected³⁶. Repeat experiments with the same sample yielded correlation values of $r^2 > 0.99$ (for both independent replicates and sequencing chip replicates). The HAM sample from donor D17 at 2 h and 72 h yielded <1 million reads and was excluded from the analyses. The AmpliSeq reads were normalized to mapped fragments per million reads for quantifying transcript expression levels⁶⁶, yielding relative abundance for predicted transcripts in each HAM.

Differentially expressed (DE) genes between control and *M.tb*-infected HAMs

To identify DE genes, we employed DESeq2⁶⁷. FDR adjusted p -values of 0.05 were used as a cutoff for identifying DE genes at each time point. We estimated size factors using the “poscount” approach to correct for different sequencing depth and performed independent analysis at each time point, specifying the individual/donor and condition (infected or control) in the model.

Detection of genes with variable expression (VE) in control and *M.tb*-infected HAMs, characterized by variance measures

To identify the most variably expressed (VE) RNAs separately in control HAMs and in those after *M.tb* infection, all HAM transcriptome data at each time point were subjected to Levene’s test⁶⁸, with ratios of variances as test statistics, yielding the reported adjusted p -value (FDR) for selected RNAs. A second variability test assesses whether the entropy of a given RNA’s expression is higher than expected given the total entropy in the *M.tb*-infected HAMs⁶⁹. A permutation test yields p -values for significance of the entropy computations.

Gene pathway and ontology analysis

We performed over representation analysis of gene ontology (GO) terms and reactome pathways using WebGestalt⁷⁰ taking the relevant gene lists for each comparison as an input and using default parameters. We retained GO terms or pathways which reached an FDR corrected p -value of 0.05. Comparison to genes associated with M1 and M2 states was performed using a curated list of genes from Viola et al.⁷¹ and Li et al.⁷².

Replication study of HAMs from a South Africa cohort

HAMs were collected from 9 close contacts of TB patients ($n = 9$) in Cape Town, South Africa (Table 2), under the approval of the Health Research Ethics Committee of Stellenbosch University. The informed consent from each donor was obtained and all ethical regulations relevant to human research participants were followed. Close contacts were defined as individuals who shared a closed space with a newly diagnosed TB patient for at least 5 h per week (all contacts were QuantiFERON positive). These TB household close contacts were used as healthy controls. The processing of BAL fluid to isolate HAMs and their downstream uses were performed as described above for the main cohort from Columbus, Ohio with minor variations. HAMs were adhered and cultured in 96-well plate (1.3×10^5 cells/well, in triplicate) in RPMI medium containing 20% human AB serum. Cells were infected with wild-type *M.tb* H₃₇R_v at an MOI of 1:1. CFU, RNA, and protein were estimated at 2, 24 and 72 h.

HAM samples were initially stored in RNAlater and transferred to TRIzol prior to shipment. RNA was isolated using Quick-RNA Microprep Kit (R1050; Zymo Research) as per the manufacturer’s instructions. Isolated RNA was quantified using the Qubit RNA High Sensitivity Assay Kit (Q32852) and Qubit 4 Fluorometer (both from ThermoFisher Scientific). Before doing RNA sequencing, RNA quality was assessed with the Fragment analyzer (Agilent). Samples with an RNA integrity number (RIN) higher than 7 were used for RNA-Seq. RNA-Seq libraries were prepared from 25 to 500 ng of total RNA using the NEB Next directional RNA library preparation Kit with poly (A) enrichment module (Ipswich, MA). RNA sequencing was carried out at the Genome Sequencing Facility (GSF) at UT Health San Antonio using the HiSeq 3000 platform (Illumina), with 50 bp single read sequencing with approximately 25 M reads per sample.

The analyses of RNA-Seq data of the South African cohort samples were carried out using CLC Genomics Workbench 22⁷³. Low-quality sequences and adapters were trimmed. Trimmed reads were mapped to the human hg38 reference genome. The reads were assigned to the transcripts using the EM algorithm. The TMM normalization⁷⁴ in EdgeR^{75,76} and multi-factorial statistics based on a negative binomial Generalized Linear Model (GLM) were carried out for differential expression analysis. Genes with FDR-adjusted p -values < 0.05 were considered to be statistically significant. Gene Set Enrichment Analysis (GSEA)⁷⁷ and KOBAS analysis⁷⁸ were carried out to identify over-represented GO terms and biological pathways.

Statistics and reproducibility

Differential protein secretion between infected and uninfected control HAMs were analyzed using non-parametric Wilcoxon tests. Transcriptome profiles of control and infected macrophages for 2, 24, and 72 h were analyzed using the Wald test in DESeq2 and presented as log2 fold change in Figs. 3 and 4. Correlations of expression of *IDO1* with several tightly expressed VE genes in Fig. 5 were analyzed by linear regression. The correlation between protein secretion at 2 h and VE mRNA expression at 24 h by both control and infected cells in Fig. 7 was estimated using the Pearson correlation coefficient (r , where 0 indicates no correlation and 1 indicates a perfect positive correlation), and p values corrected using the FDR approach. Unless otherwise stated, Student’s t tests were used to perform statistical analysis of comparisons. Significance was determined at p values indicated in the figure legends. NS: no significance at $p > 0.05$; * $p < 0.05$, ** $p < 0.01$, *** $p < 0.001$, and **** $p < 0.0001$: statistically significant at the level as indicated.

Reporting summary

Further information on research design is available in the Nature Portfolio Reporting Summary linked to this article.

Data availability

Source data for Fig. 1 can be found in Supplementary Table 1. Source data for Fig. 2 can be found in Supplementary Table 2. Source data for Figs. 3 and 4 can be found in Supplementary Table 3. Source data for Fig. 6 can be found in Supplementary Table 4A. Source data for Fig. 7 can be found in Supplementary Table 5 (Cor 2 h Protein 24 h RNA VEGs & Pval 2 h Protein 24 h RNA VEGs). The RNA sequencing data were deposited into the GEO database under accession numbers GSE189996 and GSE223863.

Received: 22 September 2023; Accepted: 4 June 2025;

Published online: 23 June 2025

References

1. WHO. *Global tuberculosis report* (World Health Organization, 2023).
2. Slood, R., Schim van der Loeff, M. F., Kow, P. M. & Borgdorff, M. W. Risk of tuberculosis after recent exposure. A 10-year follow-up study of contacts in Amsterdam. *Am. J. Respir. Crit. Care Med* **190**, 1044–1052 (2014).
3. Trauer, J. M. et al. Risk of active tuberculosis in the five years following infection ... 15%? *Chest* **149**, 516–525 (2016).
4. Azad, A. K., Lloyd, C., Sadee, W. & Schlesinger, L. S. Challenges of immune response diversity in the human population concerning new tuberculosis diagnostics, therapies, and vaccines. *Front. Cell Infect. Microbiol.* **10**, 139 (2020).
5. Guirado, E., Schlesinger, L. S. & Kaplan, G. Macrophages in tuberculosis: friend or foe. *Semin. Immunopathol.* **35**, 563–583 (2013).
6. Rajaram, M. V., Ni, B., Dodd, C. E. & Schlesinger, L. S. Macrophage immunoregulatory pathways in tuberculosis. *Semin. Immunol.* **26**, 471–485 (2014).
7. Schorey, J. S. & Schlesinger, L. S. Innate immune responses to tuberculosis. *Microbiol. Spectr.* **4**, <https://doi.org/10.1128/microbiolspec.TB2-0010-2016> (2016).
8. Pai, M. et al. Tuberculosis. *Nat. Rev. Dis. Prim.* **2**, 16076 (2016).
9. Finan, C., Ota, M. O., Marchant, A. & Newport, M. J. Natural variation in immune responses to neonatal *Mycobacterium bovis* Bacillus

- Calmette-Guerin (BCG) vaccination in a cohort of Gambian infants. *PLoS One* **3**, e3485 (2008).
10. Colditz, G. A. et al. Efficacy of BCG vaccine in the prevention of tuberculosis: Meta-analysis of the published literature. *JAMA* **271**, 698–702 (1994).
 11. Sousa, J. et al. Mycobacterium tuberculosis associated with severe tuberculosis evades cytosolic surveillance systems and modulates IL-1 β production. *Nat. Commun.* **11**, 1949 (2020).
 12. Liu, C. H., Liu, H. & Ge, B. Innate immunity in tuberculosis: host defense vs pathogen evasion. *Cell Mol. Immunol.* **14**, 963–975 (2017).
 13. Azad, A. K. et al. Allelic mRNA expression imbalance in C-type lectins reveals a frequent regulatory SNP in the human surfactant protein A (SP-A) gene. *Genes Immun.* **14**, 99–106 (2013).
 14. Azad, A. K., Sadee, W. & Schlesinger, L. S. Innate immune gene polymorphisms in tuberculosis. *Infect. Immun.* **80**, 3343–3359 (2012).
 15. Thuong, N. T. et al. Identification of tuberculosis susceptibility genes with human macrophage gene expression profiles. *PLoS Pathog.* **4**, e1000229 (2008).
 16. Barreiro, L. B. et al. Deciphering the genetic architecture of variation in the immune response to Mycobacterium tuberculosis infection. *Proc. Natl. Acad. Sci. USA* **109**, 1204–1209 (2012).
 17. Moores, R. C., Briha, S., Schutgens, F., Elkington, P. T. & Friedland, J. S. Epigenetic regulation of matrix metalloproteinase-1 and -3 expression in Mycobacterium tuberculosis Infection. *Front. Immunol.* **8**, 602 (2017).
 18. Rajaram, M. V. et al. Mycobacterium tuberculosis lipomannan blocks TNF biosynthesis by regulating macrophage MAPK-activated protein kinase 2 (MK2) and microRNA miR-125b. *Proc. Natl. Acad. Sci. USA* **108**, 17408–17413 (2011).
 19. Naranbhai, V. The role of host genetics (and genomics) in tuberculosis. *Microbiol. Spectr.* **4**, <https://doi.org/10.1128/microbiolspec.TB2-0011-2016> (2016).
 20. Uren, C. et al. A post-GWAS analysis of predicted regulatory variants and tuberculosis susceptibility. *PLoS One* **12**, e0174738 (2017).
 21. Lavalett, L. et al. Alveolar macrophages from tuberculosis patients display an altered inflammatory gene expression profile. *Tuberculosis* **107**, 156–167 (2017).
 22. Roy, S. et al. Transcriptional landscape of Mycobacterium tuberculosis infection in macrophages. *Sci. Rep.* **8**, 6758 (2018).
 23. Rothchild, A. C. et al. Alveolar macrophages generate a noncanonical NRF2-driven transcriptional response to Mycobacterium tuberculosis in vivo. *Sci. Immunol.* **4**, <https://doi.org/10.1126/sciimmunol.aaw6693> (2019).
 24. Moreira-Teixeira, L. et al. Mouse transcriptome reveals potential signatures of protection and pathogenesis in human tuberculosis. *Nat. Immunol.* **21**, 464–476 (2020).
 25. Blischak, J. D., Tailleux, L., Mitrano, A., Barreiro, L. B. & Gilad, Y. Mycobacterial infection induces a specific human innate immune response. *Sci. Rep.* **5**, 16882 (2015).
 26. Wu, K. et al. A derived network-based interferon-related signature of human macrophages responding to Mycobacterium tuberculosis. *Biomed. Res. Int.* **2014**, 713071 (2014).
 27. Bragina, E. Y., Tiys, E. S., Rudko, A. A., Ivanisenko, V. A. & Freidin, M. B. Novel tuberculosis susceptibility candidate genes revealed by the reconstruction and analysis of associative networks. *Infect. Genet. Evol.* **46**, 118–123 (2016).
 28. Campo, M. et al. Human alveolar and monocyte-derived human macrophage responses to Mycobacterium tuberculosis. *J. Immunol.* **213**, 161–169 (2024).
 29. Adu-Gyamfi, C. G. et al. Plasma indoleamine 2, 3-dioxygenase, a biomarker for tuberculosis in human immunodeficiency virus-infected patients. *Clin. Infect. Dis.* **65**, 1356–1358 (2017).
 30. Gautam, U. S. et al. In vivo inhibition of tryptophan catabolism reorganizes the tuberculoma and augments immune-mediated control of Mycobacterium tuberculosis. *Proc. Natl. Acad. Sci. USA* **115**, E62–E71 (2018).
 31. Zak, D. E. et al. A blood RNA signature for tuberculosis disease risk: a prospective cohort study. *Lancet* **387**, 2312–2322 (2016).
 32. Andreu, N. et al. Optimisation of bioluminescent reporters for use with mycobacteria. *PLoS ONE* **5**, e10777 (2010).
 33. Salunke, S. B. et al. Design and synthesis of novel anti-tuberculosis agents from the celecoxib pharmacophore. *Bioorg. Med. Chem.* **23**, 1935–1943 (2015).
 34. Guirado, E. et al. Characterization of host and microbial determinants in individuals with latent tuberculosis infection using a human granuloma model. *MBio* **6**, e02537–02514 (2015).
 35. Arnett, E. et al. PPAR γ is critical for Mycobacterium tuberculosis induction of Mcl-1 and limitation of human macrophage apoptosis. *PLoS Pathog.* **14**, e1007100 (2018).
 36. Papp, A. C. et al. AmpliSeq transcriptome analysis of human alveolar and monocyte-derived macrophages over time in response to Mycobacterium tuberculosis infection. *PLoS One* **13**, e0198221 (2018).
 37. Recio, C. et al. Activation of the immune-metabolic receptor GPR84 enhances inflammation and phagocytosis in macrophages. *Front. Immunol.* **9**, 1419 (2018).
 38. Yunna, C., Mengru, H., Lei, W. & Weidong, C. Macrophage M1/M2 polarization. *Eur. J. Pharm.* **877**, 173090 (2020).
 39. Orecchioni, M., Ghosheh, Y., Pramod, A. B. & Ley, K. Macrophage polarization: different gene signatures in M1(LPS+) vs. classically and M2(LPS-) vs. alternatively activated macrophages. *Front. Immunol.* **10**, 1084 (2019).
 40. Xue, J. et al. Transcriptome-based network analysis reveals a spectrum model of human macrophage activation. *Immunity* **40**, 274–288 (2014).
 41. Stouch, A. N. et al. IkappaB kinase activity drives fetal lung macrophage maturation along a non-M1/M2 paradigm. *J. Immunol.* **193**, 1184–1193 (2014).
 42. Mitsi, E. et al. Human alveolar macrophages predominately express combined classical M1 and M2 surface markers in steady state. *Respir. Res.* **19**, 66 (2018).
 43. Hussell, T. & Bell, T. J. Alveolar macrophages: plasticity in a tissue-specific context. *Nat. Rev. Immunol.* **14**, 81–93 (2014).
 44. Pahari, S. et al. A new tractable method for generating human alveolar macrophage-like cells in vitro to study lung inflammatory processes and diseases. *mBio* **14**, e0083423 (2023).
 45. Philips, J. A. & Ernst, J. D. Tuberculosis pathogenesis and immunity. *Annu. Rev. Pathol.* **7**, 353–384 (2012).
 46. Xue, Z. T., Sjogren, H. O., Salford, L. G. & Widegren, B. An epigenetic mechanism for high, synergistic expression of indoleamine 2,3-dioxygenase 1 (IDO1) by combined treatment with zebularine and IFN- γ : potential therapeutic use in autoimmune diseases. *Mol. Immunol.* **51**, 101–111 (2012).
 47. Li, X. et al. Detecting differentially variable microRNAs via model-based clustering. *Int. J. Genomics* **2018**, 6591634 (2018).
 48. Mayer-Barber, K. D. et al. Caspase-1 independent IL-1 β production is critical for host resistance to mycobacterium tuberculosis and does not require TLR signaling in vivo. *J. Immunol.* **184**, 3326–3330 (2010).
 49. Krishnan, N., Robertson, B. D. & Thwaites, G. Pathways of IL-1 β secretion by macrophages infected with clinical Mycobacterium tuberculosis strains. *Tuberculosis* **93**, 538–547 (2013).
 50. Sabir, N., Hussain, T., Mangi, M. H., Zhao, D. & Zhou, X. Matrix metalloproteinases: expression, regulation and role in the immunopathology of tuberculosis. *Cell Prolif.* **52**, e12649 (2019).
 51. Kang, P. B. et al. The human macrophage mannose receptor directs Mycobacterium tuberculosis lipoarabinomannan-mediated phagosome biogenesis. *J. Exp. Med.* **202**, 987–999 (2005).
 52. Penn-Nicholson, A. et al. RISK6, a 6-gene transcriptomic signature of TB disease risk, diagnosis and treatment response. *Sci. Rep.* **10**, 8629 (2020).

53. Du, M. X., Sotero-Esteve, W. D. & Taylor, M. W. Analysis of transcription factors regulating induction of indoleamine 2,3-dioxygenase by IFN- γ . *J. Interferon Cytokine Res.* **20**, 133–142 (2000).
54. Chai, Q. et al. A bacterial phospholipid phosphatase inhibits host pyroptosis by hijacking ubiquitin. *Science* **378**, eabq0132 (2022).
55. Shariq, M. et al. The exploitation of host autophagy and ubiquitin machinery by Mycobacterium tuberculosis in shaping immune responses and host defense during infection. *Autophagy* **19**, 3–23 (2023).
56. Pahari, S. et al. Protocol to develop human alveolar macrophage-like cells from mononuclear cells or purified monocytes for use in respiratory biology research. *STAR Protoc.* **5**, 103061 (2024).
57. Neehus, A. L. et al. Human inherited CCR2 deficiency underlies progressive polycystic lung disease. *Cell* **187**, 390–408 e323 (2024).
58. Arias, A. A. et al. Tuberculosis in otherwise healthy adults with inherited TNF deficiency. *Nature* **633**, 417–425 (2024).
59. Stein, M., Keshav, S., Harris, N. & Gordon, S. Interleukin 4 potently enhances murine macrophage mannose receptor activity: A marker of alternative immunologic macrophage activation. *J. Exp. Med.* **176**, 287–292 (1992).
60. Refai, A., Gritli, S., Barbouche, M. R. & Essafi, M. Mycobacterium tuberculosis virulent factor ESAT-6 drives macrophage differentiation toward the pro-inflammatory m1 phenotype and subsequently switches it to the anti-inflammatory M2 phenotype. *Front. Cell Infect. Microbiol.* **8**, 327 (2018).
61. Tameris, M. D. et al. Safety and efficacy of MVA85A, a new tuberculosis vaccine, in infants previously vaccinated with BCG: a randomised, placebo-controlled phase 2b trial. *Lancet* **381**, 1021–1028 (2013).
62. Gaynor, C. D., McCormack, F. X., Voelker, D. R., McGowan, S. E. & Schlesinger, L. S. Pulmonary surfactant protein A mediates enhanced phagocytosis of Mycobacterium tuberculosis by a direct interaction with human macrophages. *J. Immunol.* **155**, 5343–5351 (1995).
63. Nguyen, H. A., Rajaram, M. V., Meyer, D. A. & Schlesinger, L. S. Pulmonary surfactant protein A and surfactant lipids upregulate IRAK-M, a negative regulator of TLR-mediated inflammation in human macrophages. *Am. J. Physiol. Lung Cell Mol. Physiol.* **303**, L608–L616 (2012).
64. Schlesinger, L. S., Bellingerkawahara, C. G., Payne, N. R. & Horwitz, M. A. Phagocytosis of Mycobacterium-tuberculosis is mediated by human monocyte complement receptors and complement component-C3. *J. Immunol.* **144**, 2771–2780 (1990).
65. Johnson, W. E., Li, C. & Rabinovic, A. Adjusting batch effects in microarray expression data using empirical Bayes methods. *Biostatistics* **8**, 118–127 (2007).
66. Mortazavi, A., Williams, B. A., McCue, K., Schaeffer, L. & Wold, B. Mapping and quantifying mammalian transcriptomes by RNA-Seq. *Nat. Methods* **5**, 621–628 (2008).
67. Love, M. I., Huber, W. & Anders, S. Moderated estimation of fold change and dispersion for RNA-seq data with DESeq2. *Genome Biol.* **15**, 550 (2014).
68. Levene, H. In *Contributions to probability and statistics* (ed Hotelling, H. et al.) 278–292 (Stanford University Press, 1960).
69. Handelman, S. K. et al. Conditional entropy in variation-adjusted windows detects selection signatures associated with expression quantitative trait loci (eQTLs). *BMC Genomics* **16**, S8 (2015).
70. Liao, Y., Wang, J., Jaehnig, E. J., Shi, Z. & Zhang, B. WebGestalt 2019: gene set analysis toolkit with revamped UIs and APIs. *Nucleic Acids Res.* **47**, W199–W205 (2019).
71. Viola, A., Munari, F., Sanchez-Rodriguez, R., Scolaro, T. & Castegna, A. The metabolic signature of macrophage responses. *Front. Immunol.* **10**, 1462 (2019).
72. Li, P. et al. Comparative proteomic analysis of polarized human THP-1 and Mouse RAW264.7 macrophages. *Front. Immunol.* **12**, 700009 (2021).
73. Liu, C. H. & Di, Y. P. Analysis of RNA sequencing data using CLC genomics workbench. *Methods Mol. Biol.* **2102**, 61–113 (2020).
74. Robinson, M. D. & Oshlack, A. A scaling normalization method for differential expression analysis of RNA-seq data. *Genome Biol.* **11**, R25 (2010).
75. McCarthy, D. J., Chen, Y. & Smyth, G. K. Differential expression analysis of multifactor RNA-Seq experiments with respect to biological variation. *Nucleic Acids Res.* **40**, 4288–4297 (2012).
76. Robinson, M. D., McCarthy, D. J. & Smyth, G. K. edgeR: a Bioconductor package for differential expression analysis of digital gene expression data. *Bioinformatics* **26**, 139–140 (2010).
77. Mootha, V. K. et al. PGC-1 α -responsive genes involved in oxidative phosphorylation are coordinately downregulated in human diabetes. *Nat. Genet.* **34**, 267–273 (2003).
78. Bu, D. et al. KOBAS-i: intelligent prioritization and exploratory visualization of biological functions for gene enrichment analysis. *Nucleic Acids Res.* **49**, W317–W325 (2021).

Acknowledgements

We acknowledge the use of the Bio-Safety Level 3 (BSL3) facility at the OSU for *M.tb* infection of human HAMs and Genome Sequencing Facility at UT Health San Antonio for the RNA-Seq study in this project. This study was supported in part by a grant from the Bill & Melinda Gates Foundation, the National Research Foundation of South Africa (RDYR14072278217) and grants from the National Institutes of Health (NIH): General Medical Sciences U01 GM092655 and R01 AI136831 National Institute of Allergy and Infectious Diseases (NIAID) and the South African Medical Research Council under the US-South African Program for Collaborative Biomedical Research (R01AI116039). Genome Sequencing Facility at UT Health San Antonio is supported by UT Health San Antonio, NIH-NCI P30 CA054174 (Cancer Center at UT Health San Antonio), NIH Shared Instrument grant S10OD030311 (S10 grant to NovaSeq 6000 System), and CPRIT Core Facility Award (RP220662).

Author contributions

L.S.S. and W.S. conceived and designed the study. H.M.C., E.A., and M.D.W. contributed to acquiring ethics approval and human samples. A.K.A., A.P., and A.M.W. performed experiments and data analysis. I.H.C. and A.P. contributed to data visualization and figure preparation. S.L., X.Z., and M.S. performed bio-statistical analyses. Y.W., H.Z., H.C., and M.P. performed bioinformatics analyses. B.I.R., L.K., K.R., C.K., H.T., and G.W. contributed to replication study. W.S., L.S.S., I.H.C., A.K.A., and E.A. wrote the manuscript with input from all coauthors. All authors read, edited, and approved of the revised final manuscript.

Competing interests

The authors declare no competing interests.

Additional information

Supplementary information The online version contains supplementary material available at <https://doi.org/10.1038/s42003-025-08337-9>.

Correspondence and requests for materials should be addressed to Wolfgang Sadee or Larry S. Schlesinger.

Peer review information *Communications Biology* thanks Anna Coussens and the other, anonymous, reviewers for their contribution to the peer review of this work. Primary Handling Editors: Kaiwen Chen and Johannes Stortz.

Reprints and permissions information is available at <http://www.nature.com/reprints>

Publisher's note Springer Nature remains neutral with regard to jurisdictional claims in published maps and institutional affiliations.

Open Access This article is licensed under a Creative Commons Attribution-NonCommercial-NoDerivatives 4.0 International License, which permits any non-commercial use, sharing, distribution and reproduction in any medium or format, as long as you give appropriate credit to the original author(s) and the source, provide a link to the Creative Commons licence, and indicate if you modified the licensed material. You do not have permission under this licence to share adapted material derived from this article or parts of it. The images or other third party material in this article are included in the article's Creative Commons licence, unless indicated otherwise in a credit line to the material. If material is not included in the article's Creative Commons licence and your intended use is not permitted by statutory regulation or exceeds the permitted use, you will need to obtain permission directly from the copyright holder. To view a copy of this licence, visit <http://creativecommons.org/licenses/by-nc-nd/4.0/>.

© The Author(s) 2025